

Enhancement of dispersion and bonding of graphene-polymer through wet transfer of functionalized graphene oxide

M. Moazzami Gudarzi, F. Sharif*

Department of Polymer Engineering and Color Technology, Amirkabir University of Technology, Tehran, Iran

Received 20 May 2012; accepted in revised form 29 July 2012

Abstract. Dispersion of nanomaterials in polymeric matrices plays an important role in determining the final properties of the composites. Dispersion in nano scale, and especially in single layers, provides best opportunity for bonding. In this study, we propose that by proper functionalization and mixing strategy of graphene its dispersion, and bonding to the polymeric matrix can be improved. We then apply this strategy to graphene-epoxy system by amino functionalization of graphene oxide (GO). The process included two phase extraction, and resulted in better dispersion and higher loading of graphene in epoxy matrix. Rheological evaluation of different graphene-epoxy dispersions showed a rheological percolation threshold of 0.2 vol% which is an indication of highly dispersed nanosheets. Observation of the samples by optical microscopy, scanning electron microscopy (SEM), and atomic force microscopy (AFM), showed dispersion homogeneity of the sheets at micro and nano scales. Study of graphene-epoxy composites showed good bonding between graphene and epoxy. Mechanical properties of the samples were consistent with theoretical predictions for ideal composites indicating molecular level dispersion and good bonding between nanosheets and epoxy matrix.

Keywords: nanocomposites, graphene, epoxy, functionalization, rheology

1. Introduction

Carbon nanomaterials have emerged as a rising star in the material science community, during the past two decades [1–3]. Exceptional physical and mechanical properties of carbon nanomaterials can be incorporated into polymers resulting in composite materials with improved properties [4, 5]. Hybridization of carbon nanomaterials and polymers has led to the production of composites with enhanced electrical and mechanical properties for new applications such as solar cells [6], electromagnetic interference shielding [7], and sensors [8].

Due to the high surface area, nanofillers tend to agglomerate and stick to each other, forming micro particles [9, 10]. Therefore, dispersion of nanofiller into individual particles throughout the matrix,

especially molecular level dispersion, is an essential step [10]. Agglomeration is even more severe for anisotropic nanoparticles such as nanotubes and nanosheets due to the high interparticle interaction. Emerging graphene and its derivatives as fillers for polymeric materials has led to the production of a new class of nanocomposites [5, 11]. Remarkable improvements in physical and mechanical properties of polymer have been reported upon addition of a small amount of graphene [11, 12]. Similar to other layered nanofillers, graphene sheets are prone to restacking due to the high aspect ratio and strong interparticle interaction [11]. Although, chemically derived graphene is available as single layer dispersion in liquids, retaining the single layer state of graphene in polymer media is not easy [11–13].

*Corresponding author, e-mail: sharif@aut.ac.ir
© BME-PT

Chemically derived graphene is commonly produced by oxidizing graphite to graphite oxide with a layered hydrophilic structure, which is then exfoliated into the graphene oxide (GO) in aqueous media or polar solvents, possibly by mechanical shearing [14, 15]. Because of the hydrophilic nature of GO, it is not easily dispersed in weakly polar organic solvents, and polymers [16]. Reduction of GO usually results in serve aggregation of reduced GO (rGO) [11].

Many attempts have been made to disperse chemically derived graphene in low polarity organic media by functionalization of GO. However; employing aqueous dispersion of GO to fabricate graphene-based composite is more attractive, since it can be easily combined with water soluble polymers and then reduced to rGO [17] without using organic solvents or chemical functionalization which can be toxic and/or costly [18–20].

Furthermore, colloidal polymer particles may be mixed with GO to incorporate graphene into non-water soluble polymers [21–24]. Our recent study also shows GO can be employed as a surfactant in emulsion polymerization to produce polymer-graphene nanocomposites [25]. Therefore it is a practical and environmentally friendly strategy, to use aqueous dispersion of GO to produce polymer graphene and GO composites.

In this paper we have used the case of epoxy-functionalized GO to address the challenges of well dispersing graphenic sheets in a thermoset resin and show the success of the proposed strategy. Fabrication of epoxy composites with grapheme, GO, and functionalized graphene is mostly performed through [26–31]:

- i) Dispersion of graphene (obtained via different chemical pathways including thermal expansion of graphite oxide) in organic solvents such as acetone [27, 31]
- ii) Multi-step chemical functionalization of graphene (oxide) and then removing solvent from the mixture of epoxy and graphene [28].

Direct mixing of graphenic powder in viscous epoxy resin usually results in poor dispersion. It should be noted that even ultrasonication of graphenic sheets in organic solvent for a long period of time does not guarantee a good dispersion especially for higher graphenic contents [28]. On the other hand, GO sheets easily restack during drying, and form a layered material consisting of GO sheets that are

strongly bonded together by hydrogen bonding [32]. To ensure well dispersion of GO in polymer, restacking of the graphenic sheets must be avoided.

Recently, Li and coworkers [33, 34] uncovered that in ‘wet’ graphenic sheets, water acts as ‘spacer’ keeping the nanosheets separated. Therefore, wet transfer of GO into organic phase, *i.e.* epoxy resin, can prevent restacking and agglomeration of nanolayers [33–35].

In addition to good dispersion, we need to ensure good GO-matrix bonding, to obtain superior mechanical properties [28, 36]. In the next section we describe a novel and single-step method to functionalize and disperse GO nanosheets in epoxy and obtain high performance nanocomposites by achieving a high degree of dispersion and good bonding to the matrix.

Although graphite oxide has been synthesised long ago, its exact molecular structure is not well known [17–19, 37]. However, presence of epoxy and carboxyl groups has been confirmed [16]. Presence of epoxy groups is valuable as they facilitate the GO functionalization, compared to other groups such as the carboxyl group which needs activation in the absence of water [16]. Strong nucleophilic agents such as amines can readily react with the epoxy group through a ring opening reaction without any activation. Therefore, amines have extensively been employed for the functionalization of GO [16]. The reaction is carried out in aqueous media and ambient atmosphere without catalyst. The reaction is relatively fast, due to the high reactivity of amine and epoxy groups.

Amino functionalization of carbon nanotubes (CNTs) has been extensively used to improve interfacial interaction with epoxy matrices [38–40]. In analogy to CNTs, covalent bond formation between amino functionalized GO surface and epoxy resin is anticipated [41, 42].

The method serves two simultaneous purposes of accommodating graphenic sheets at the molecular level and furnishing the interfacial bonding with the matrix which are highly desirable. Higher dispersion means higher area per volume and better bonding means efficient use of filler presence in the matrix to improve mechanical properties. Direct impact of higher quality dispersion and interfacial bonding on the mechanical properties are shown to approach theoretical predictions for ideal composites.

2. Experimentals

2.1. Materials

Natural graphite flake ($<50\ \mu\text{m}$) was purchased from Merck Chemicals, Germany. Epoxy resin (diglycidyl ether of bisphenol A, Epon828) was obtained from Shell, USA. Isophoronediamine (IPDA) from Fluka, USA was used as hardener. All other reagents were purchased from Merck Chemicals, Germany and used as received.

2.2. Functionalization of GO

Graphite oxide was synthesized from natural graphite flakes using Hummers' method [20, 37]. Homogeneous dispersion of GO was obtained by sonication of the graphite oxide suspension in water for an hour and centrifuging for 10 minutes at 4000 rpm. An aromatic diamine (PPDA) was used to functionalize GO sheets to increase compatibility of GO sheets with epoxy resin, although other diamines (aliphatic or aromatic) can be used for amino-functionalization of GO through the same mixing strategy (wet transfer). The excess amount of diamine was used to ensure that at least one of the amine groups has reacted with epoxy groups on GO and have amine groups on the surface of GO. In order to functionalize GO sheets, *p*-Phenylenediamine (PPDA) was dissolved in hot water and mixed with GO suspension (2.5 mg/mL), resulting in a GO/PPDA mass ratio of 1 to 5. The mixture was then heated to 80°C for 30 minutes to complete the reaction. The result was a dark violet precipitation which was washed several times with water to remove the excess PPDA.

2.3. Preparation of nanocomposites

The functionalized GO (fGO) slurry was mixed with epoxy resin. The mixture was sonicated with a tip sonicator for 5 minutes transferring the fGO particles from water to epoxy. The water was then removed by decanting and heating at 100°C for 48 hours resulting in a dark violet epoxy-fGO. The mixture was further sonicated for 5 minutes.

The stoichiometric amount of hardener (IPDA) was added to cure the resin at room temperature for 24 hr and then post-cured at 100°C for 2 hours. Volume fractions of fGO in final composites were calculated considering the density of epoxy and graphenic sheets 1.16 and 2.2 g/cm³; respectively.

2.4. Characterization

Scanning electron microscope (SEM, LEO 1455VP, USA) was used to evaluate the morphology of graphite, graphite oxide, GO and fractured surface of the composites. A thin layer of platinum was coated on the samples to avoid electron charging.

X-ray diffraction experiments were performed at ambient temperature to study crystalline structure of materials, using an X-ray diffraction system (Philips X'Pert, Neitherland) employing CuK_α radiation (X-ray wavelength $\lambda = 1.5406\ \text{Å}$) under normal laboratory conditions.

Optical micrographs of dispersions on a transparent glass slide were taken using Leica DMR microscope, USA.

Fourier transform infrared spectroscopy (FTIR, Perkin-Elmer Spectrum One, USA) was employed to study functionalization. GO and fGO powder were molded into discs using KBr.

X-ray photoelectronic spectroscopy (XPS) was utilized to evaluate the chemical structure of the GO and fGO. The measurements were carried out by a Gamdata-scienta ESCA 200 hemispherical analyzer equipped with a monochromatic Al K_α X-ray source (X-ray wavelength $\lambda = 8.34\ \text{Å}$; $h\nu = 1486.6\ \text{eV}$), USA.

Rheological measurements were conducted in an oscillatory mode on a rheometer (Anton Paar, MCR300, Austria) equipped with parallel plate geometry. Dynamic viscoelastic material functions of the epoxy-fGO mixtures were measured as a function of frequency for small strains at room temperature. The frequency sweeps were run using strain values in the linear viscoelastic region at angular frequencies (ω) of 0.1–100 s⁻¹.

AFM pictures were taken on Dualscope DS 95-200, DME, Denmark. Samples for AFM were prepared by spin coating (2000 rpm) of aqueous dispersions of GO on a freshly cleaved mica surface. In addition, fractured surface topography of epoxy and nanocomposites was evaluated by AFM.

A three-point flexural test was used to evaluate the mechanical properties of composites. Samples were molded into 12.7 mm wide \times 70 mm long \times 3 mm thick, using silicone mold. The samples were then subjected to bending by a support span of 50 mm at a constant cross-head speed of 1 mm/min on universal testing machine Galdabini Sun 2500, Italy. Five specimens were tested for each set of conditions.

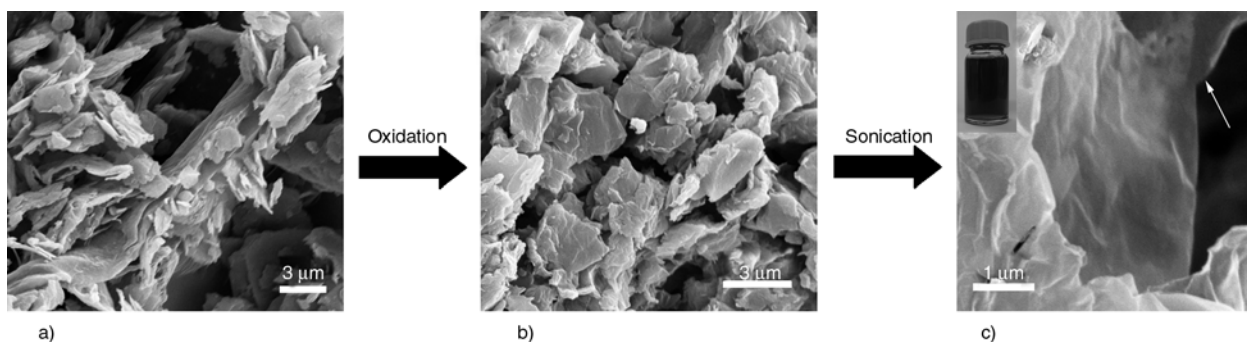


Figure 1. SEM images of (a) graphite flakes (b) graphite oxide (c) GO

3. Results and discussion

3.1. Study of GO morphology

A natural graphite flake is composed of thousands of graphene layers firmly stacked on each other. Strong oxidation of graphite converts it to a hydrophilic layered compound, *i.e.* graphite oxide [16]. Morphologies of graphite and graphite oxide, are shown in Figure 1a and 1b. Graphite flakes with few micrometers lateral size and sub-micron thickness can be observed. On the other hand, an image of graphite oxide, shows a large increase in the thickness of graphite flakes during oxidization, whereas the lateral size of flakes shows marginal decrease, which is in agreement with recent mechanism proposed by Pan and Aksay [16] that small graphite flakes are less prone to lateral cleavage. (Figure 1b). Such remarkable increase in the thickness of graphite flakes during the oxidization stems from formation of oxygen groups in the basal plane of graphite [14, 16]. In addition, the presence of oxygen groups in the structure of graphite oxide facilitates intercalation of water molecules into graphite oxide interlayer. Therefore exfoliation of

graphite oxide is not only due to the hydrophilization of graphene layers, but also because of substantial decrease in the interlayer interaction, caused by intense intercalation of the graphite oxide.

XRD was also employed to evaluate effects of oxidization on the interlayer distance of graphite. Figure 2 depicts XRD patterns of graphite and graphite oxide showing diffraction peaks at 26.58 and 11.6° for graphite and graphite oxide; respectively. This indicates intense intercalation of graphite during oxidization. Increase of d-spacing from 3.35 to

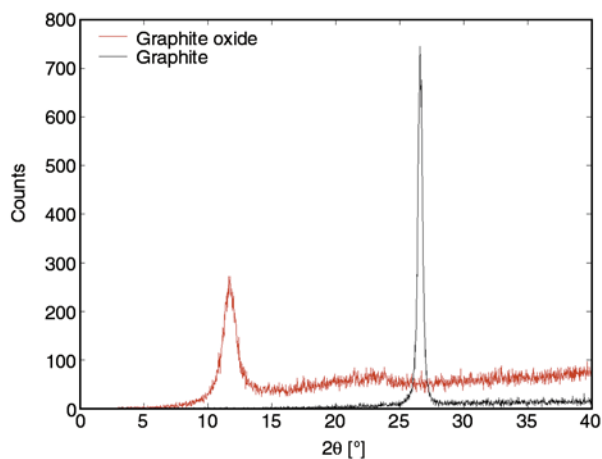


Figure 2. XRD patterns of graphite flakes and graphite oxide

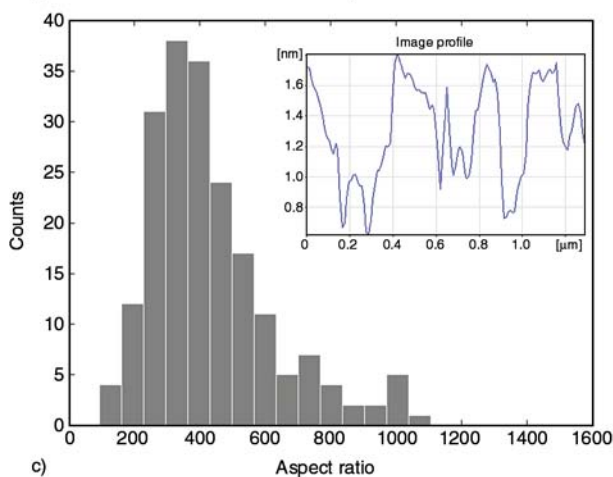
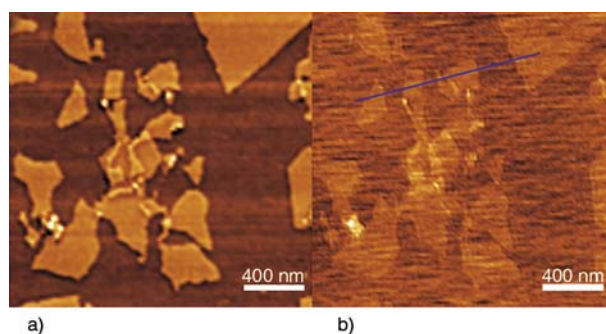


Figure 3. AFM (a) phase and (b) topograph images of graphene oxide spin coated on a mica substrate from GO dispersion in water. (c) Histogram of GO sheets aspect ratio obtained from AFM images analysis.

7.63 Å is a typical increase in the interlayer distance for oxidization of graphite [16].

Ultrasonication of aqueous slurry of graphite oxide was used to exfoliate graphite oxide flakes into GO. Exfoliation of aqueous dispersion of graphite oxide resulted in GO dispersion which was stable for months. Figure 1c shows SEM micrographs of the ultrathin GO sheets formed by exfoliation of graphite oxide. AFM was also utilized to characterize size and thickness of GO nanolayers. Figure 3b shows a typical AFM topography of GO on a mica substrate. Image analyses reveal presence of nanolayers, with a thickness of 0.7–1.5 nm and average thickness of 1 nm, indicating that the product is mostly GO monolayer [11]. On the other hand, the lateral size of GO sheets ranges from 150 to 1000 nm and average size of 380 nm. The aspect ratio of nanolayer plays a crucial role in determining the final properties of the composite; therefore, distribution of aspect ratio of the resulting GO nanolayer was obtained from AFM and presented in Figure 3c. The average aspect ratio of GO is roughly 350.

3.2. Functionalization of GO

Many researchers have employed multi-step procedures for amino functionalization of CNTs and graphene using a large amount of organic solvents. In addition, presence of some chemical groups such as acyl chloride, which are very sensitive to moisture and impurities, makes it difficult to control the reaction [38–40]. Therefore a fast and effective amino functionalization of GO through a one pot reaction with diamines is highly desirable. Similar processes have been employed for amino functionalization of clay nanosheets [43].

Figure 4 shows FTIR spectra for GO and fGO. Peaks at 3420 and 1722 cm^{-1} indicate the presence of hydroxyl and carboxyl groups in the structure of GO [41]. Epoxide groups are evidenced by the peak at 1226 cm^{-1} . The adsorption intensity is higher at the peaks of 1226 cm^{-1} in GO spectrum compared with fGO (Figure 4) which may be attributed to the reaction of epoxide groups through the ring opening [44, 45]. It should be noted, that Chen *et al.* [45] recently found that PPDA can effectively reduce GO. However, no remarkable increase in electrical conductivity of GO was observed after functionalization which implies that reduction of GO did not occur significantly. On the other hand, the intensity

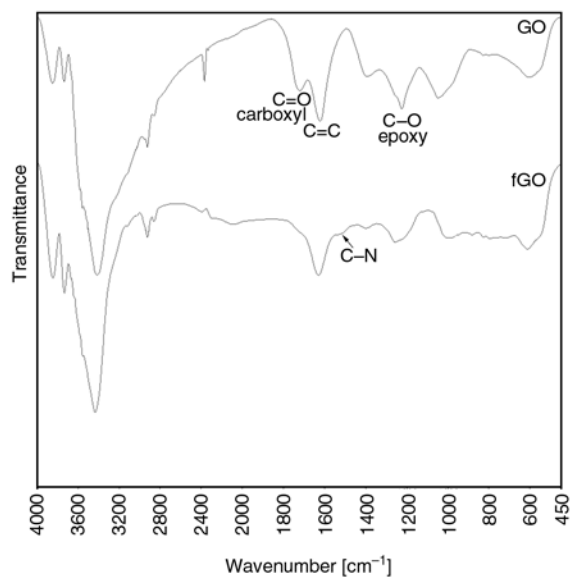


Figure 4. FTIR spectra for (a) graphite oxide powders and (b) PPDA functionalized graphene oxide powders

of the peak at 1722 cm^{-1} which is the indication of the carbonyl group (C=O), is weaker hinting to the formation of ammonium carboxylate complex [41, 44]. Furthermore, disappearance of sharp peak at 2350 cm^{-1} which is attributed to the stretching of hydroxyl of carboxyl acid groups, is another sign of formation of ammonium-carboxylate complex. There is also a new peak at 1500 cm^{-1} for fGO which is the indication of C–N bond stretch in fGO [44]. C–N bond formation can be attributed to a $\text{S}_{\text{N}}2$ nucleophilic substitution and ring opening reaction resulting in new bond formation between carbon atoms in GO and nitrogen in PPDA. In addition, attachment of PPDA moieties on the surface of GO creates some amine groups with the C–N bond.

XPS was employed to analyze the chemical structure of GO and fGO (Figure 5). Figure 5a presents the XPS spectrum of GO in the region of 0 to 800 eV. In the broad scan of the GO spectrum, presence of carbon and oxygen is confirmed with C/O ratio of 1.88. This is consistent with the reported chemical composition of GO in the literature where the C/O ratio is around 2 [14, 16]. The GO spectrum in N1s region (400 eV) reveals that the nitrogen content in the GO is less than 0.1 wt% (Figure 5b).

After GO was functionalized by PPDA, in the broad scan spectrum, a new peak around 400 eV appears which is attributed to N1s component (Figure 5c). This indicates successful amino functionalization of GO using PPDA. Amine treated GO, has C/O ratio of 2.43 which is slightly higher than GO itself. This

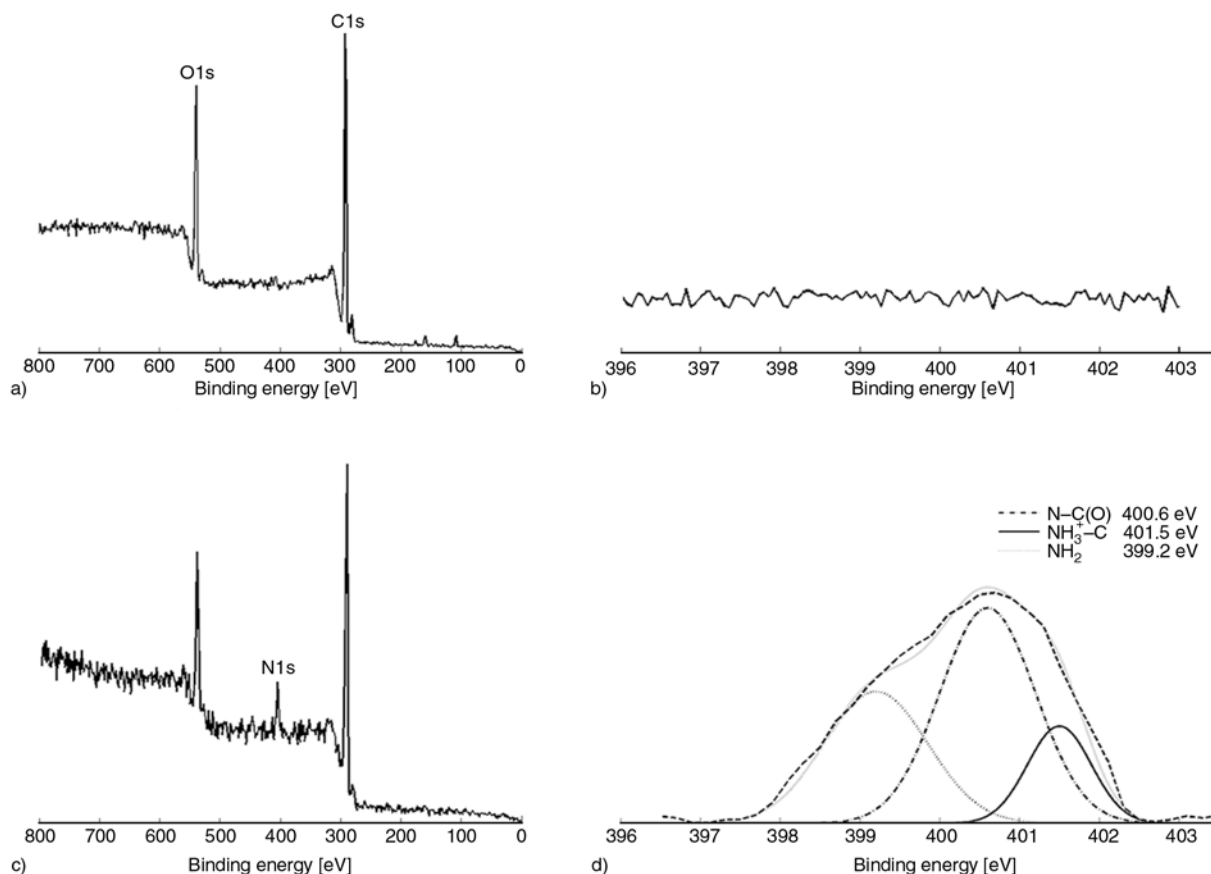


Figure 5. XPS spectra of (a, b) GO and (c, d) fGO samples, (a, c) wide region and (b, d) spectra in the N1s region

increase in C/O ratio might be attributed to incorporation of carbon atoms after functionalization by PPDA. The nitrogen content in fGO is remarkably higher, compared with GO. C/N ratio reaches to 14.5 which is similar to alkylamines modified GO [41, 42]. Considering the chemical structure of PPDA ($C_6N_2H_8$), it is realized that there is one PPDA moiety for every 23 carbon atoms in the reaction product. In addition, these analysis give $C_{2.0}O_{1.04}-(PPDA)_{0.087}$ empirical formula for the fGO. Thus, the ratio of carbon to oxygen in fGO after subtracting PPDA contribution is around 1.93 which shows no reduction during functionalization reaction indicating that no significant oxidative or polymerization reaction have occurred, in contrast to Chen *et al.* [45] report where formation of oxidized-PPDA by-products is observed. Figure 5d which is the deconvoluted N1s spectrum of fGO supports the presence of nitrogen in the forms of NH_2 (399.2 eV), $N-C(O)$ (400.6 eV), NH_3^+-C (401.5 eV). This suggests reaction of PPDA with GO through both ring opening and ammonium carboxylate formation.

As mentioned earlier aqueous GO dispersion was stable for months. However, the reaction between GO and amine results in fGO agglomeration in a few minutes. Previous studies have revealed that aqueous dispersion of GO is stable because of electrostatic stabilization resulting from ionization of carboxyl groups [15]. Destabilization of GO during the reaction with amine appears to be the result of neutralization of carboxyl ion as supported by FTIR and XPS observations [44].

Based on above observations and analyses, a scheme for functionalization is proposed (Figure 6a). Diamine molecules react with GO through a ring opening reaction and covalently graft on the surface of GO. Due to the excess amount of diamine, mostly one amine group participates in this reaction. Meanwhile, PPDA molecules form ammonium carboxylate complex with carboxyl groups in the structure of GO. Therefore, formation of amine groups at both basal plane and the edge of GO sheets is possible due to the presence of epoxy group at basal plane and carboxyl group at the edges.

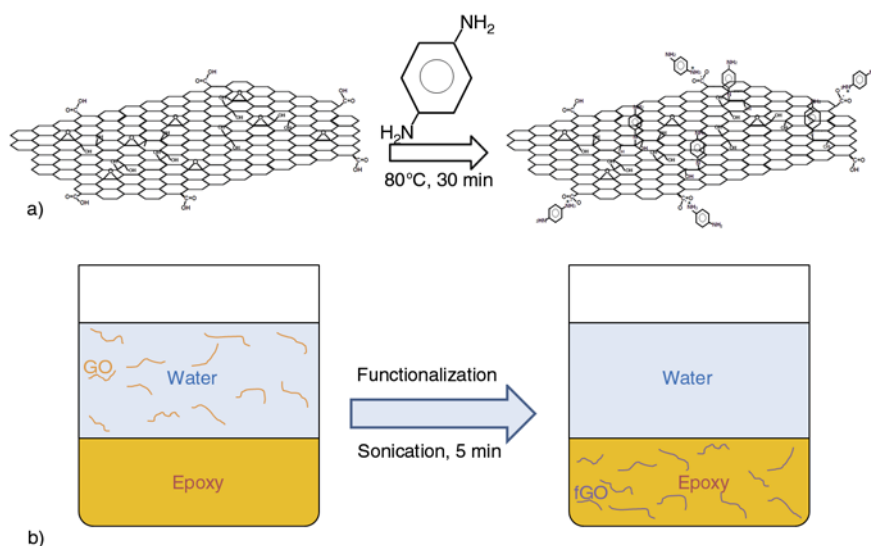


Figure 6. (a) Schematic representation diamine bonding to GO. (b) Schematic illustration of transferring GO sheets from water to epoxy phase after functionalization.

3.3. Dispersing fGO in epoxy

Immiscible ‘target’ phase, *e.g.* epoxy, and ‘transfer’ phase, *e.g.* water, were mixed to produce a mixture of highly dispersed fGO in epoxy (Figure 6b). Untreated GO sheets, which are dispersed in the transfer phase migrate to the target phase, while the reaction takes place and sheets become compatible with the epoxy. As mentioned earlier, ‘wet’ transfer of GO sheets prohibits restacking and agglomeration of nanosheets [33]. Also addition of amine to GO dispersion destabilizes the graphene sheets, aggregates of fGO are still loose since water molecules act as spacer among them. These loose aggregates are more compatible with epoxy resin due to amino-functionalization and migrate to organic phase. Our attempts fail to achieve homogeneous dispersion of fGO in epoxy when dried powder of fGO directly mixed with epoxy resin clearly illustrates the crucial role of mixing strategy to fine dispersion of graphenic sheets. This method has been employed to disperse clay [46], silica [47], and graphene [26, 48, 49] in organic media. Presence of oxygen groups, amine groups and aromatic rings in the structure of fGO, makes it compatible with epoxy resin, facilitating the dispersion of fGO sheets in epoxy and formation of possible hydrogen or covalent bonds. The result was a dark violet homogeneous dispersion of fGO in the epoxy.

Dispersion of the fGO sheets in the final mixture was studied using optical microscopy. Figure 7 shows that fGO sheets have been dispersed homo-



Figure 7. Optical microscopy images of uncured epoxy containing 0.26 vol% fGO coated on glass substrate. Inset shows a picture of the dispersion between glass slides

geneously throughout the matrix. Due to the high specific surface area of graphene sheets, they can be observed thoroughly in the micrograph, even at very low concentrations (0.26 vol%).

The quality of dispersion was also examined by SEM and shown in Figure 8. Figure 8c–8e are the SEM images of the fractured surface of the epoxy-fGO composite. Similar to the optical micrograph observations, there is no sign of agglomeration of graphene sheets. Roughness of the fractured surface

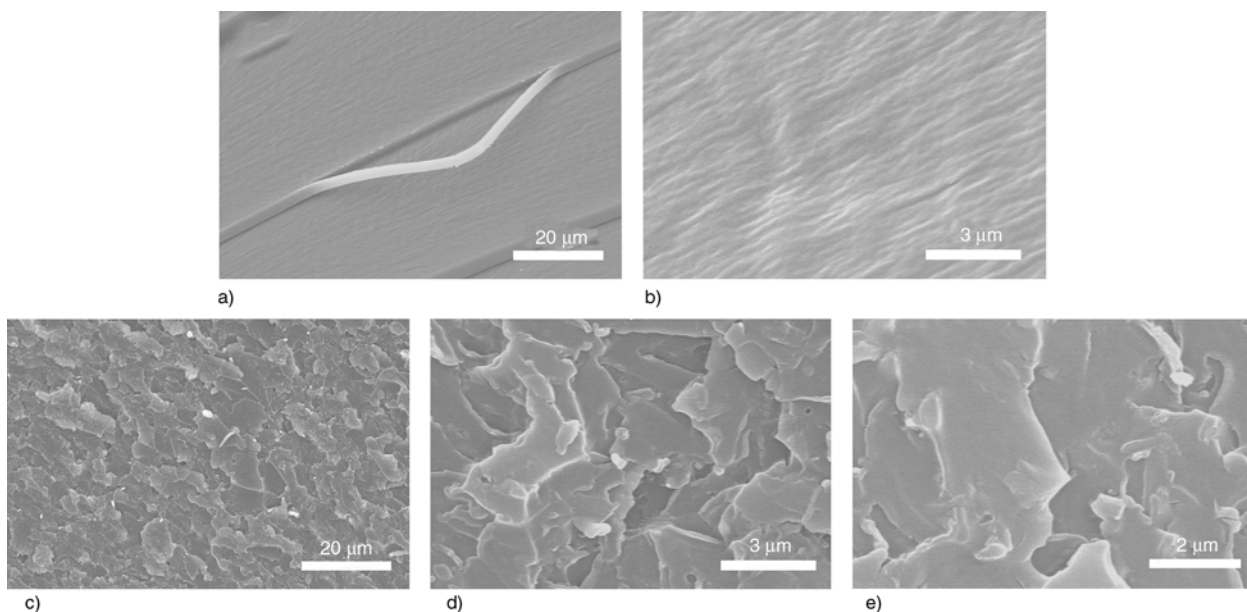


Figure 8. SEM images of fracture surface of (a, b) neat resin and (c–e) composite containing 0.2 vol% fGO at different magnifications

of the composite drastically increases upon addition of the fGO sheet to matrix compared to the neat resin, probably because of the fine dispersion of graphene sheets throughout the matrix. The fractographs of the pristine resin illustrate a very smooth surface with some stripes in the direction of fracturing force (Figure 8a and 8b). On the other hand, incorporating the fGO sheets into the matrix resulted in the formation of irregular protuberances evenly distributed in the whole fractured surface of the composites. These protuberances come into sight in the form of the bright lines with sizes of few hundreds of nanometers to few microns. Formation of these homogeneously dispersed lines arise from fine embedding of graphenic layers which are strongly bonded with epoxy matrix without any debonding or pull-out of nanolayers. The strong attachment may be attributed to the covalent bond formation between epoxy matrix and fGO sheets during the curing process. Improved dispersion and bonding of graphene sheets can significantly affect the final mechanical properties of composites [12].

Changes in fractured surface of composites, and dispersion state of graphene sheets in the matrix were also examined by AFM. Figure 9 shows topology of fracture surface of pristine epoxy and composite containing 0.2 vol% fGO. Similar to SEM analysis, the fracture surface of neat resin appears very smooth (Figure 9a). The average roughness of the resulting surface was found to be around

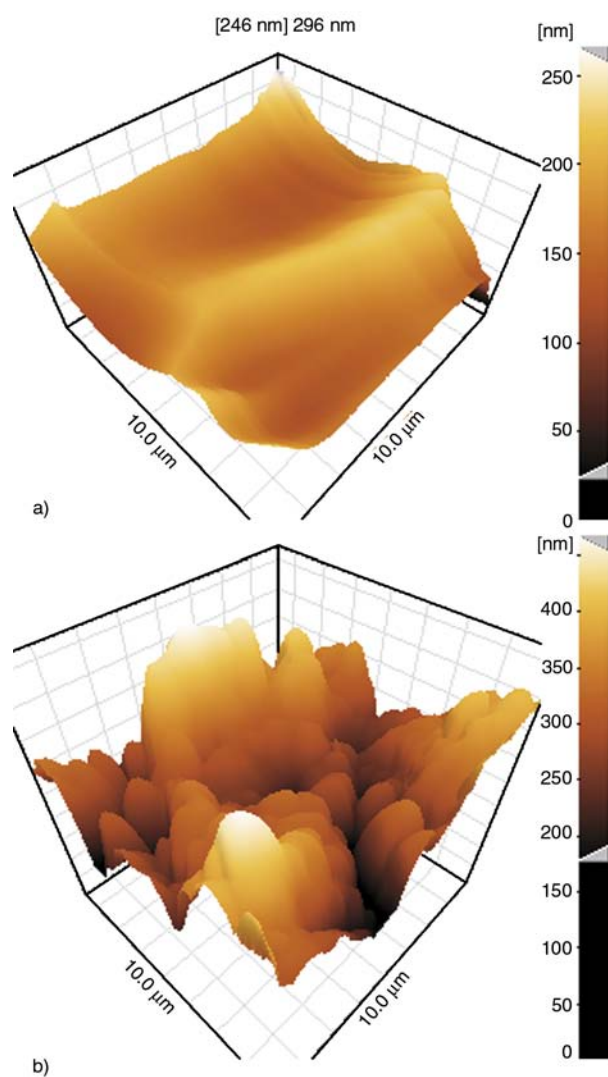


Figure 9. AFM images of fracture surface of (a) neat resin and (b) composite containing 0.4 wt% fGO

$0.03 \pm 0.01 \mu\text{m}$. On the other hand, incorporating fGO nanosheets into epoxy resin makes the fracture surface bumpy which is consistent with SEM observations (Figure 9b). The average roughness of the surface remarkably increases to $0.1 \pm 0.02 \mu\text{m}$, after addition of 0.2 vol% fGO. The increase in the surface roughness indicates induced crack deflection by graphenic sheets, during the fracture. This may improve not only the stiffness but also fracture toughness and ductility of the composite [27].

Chemical treatment of nanofillers surfaces has been widely reported to improve final properties of the composites [11, 38–40]. Recently, Rafiee *et al.* [27] has reported significant improvement in mechanical properties of the epoxy matrix by addition of a very small amount of graphene sheets. However, mechanical properties of composites diminished, as the graphene content increased to more than 0.1 wt%. The diminishing effect has been attributed to the lack of proper dispersion. Recently reported two-phase extraction method, for production of the epoxy-GO composite was not able to load graphene higher than 0.15 wt% [26], while we were able to load graphene into epoxy up to 0.5 vol% (~ 1 wt%). A recent work on fabrication of epoxy-amine rich graphene dealt with a laborious and time consuming functionalization procedure [28] whereas one can produce epoxy-GO nanocomposites through fast and facile reaction of diamines with GO, and two phase extraction method, in large scale and for industrial purposes.

Although SEM and optical microscope images demonstrate a homogeneous dispersion of the fGO sheets in the epoxy matrix, rheological measurements have been used to show that the nano sheets are dispersed as single layers.

Rheological percolation threshold of a mixture, containing anisotropic particles is inversely proportional to the aspect ratio of particles and dispersion state of the filler [11, 50–53]. For a given aspect ratio, the percolation threshold of composites decreases as dispersion of the filler improves. In addition, many models have been developed to calculate the percolation threshold of the composite system as a function of aspect ratio [50, 52]. Thus, it is possible to assess the dispersion state of filler in a composite by comparing the predicted percolation threshold and the actual one. AFM observation (Figure 3) of the samples gave an average aspect ratio of 350. For randomly oriented ellipsoids with an aspect ratio of 350 the theoretical percolation threshold is estimated to be around 0.2 vol% [50].

Figure 10a is the graph of complex viscosity of uncured epoxy composites as a function of frequency. Neat resin, and mixtures containing up to 0.05 vol% fGO, have a Newtonian behavior. For mixtures containing 0.16 vol% of fGO, a shear thinning behavior is observed. The flow index reaches to 0.7 for 0.26 vol% accompanied by a significant increase in complex viscosity. Storage modulus of resin increases by addition of the filler (Figure 10b). At low frequency, storage modulus (G') significantly

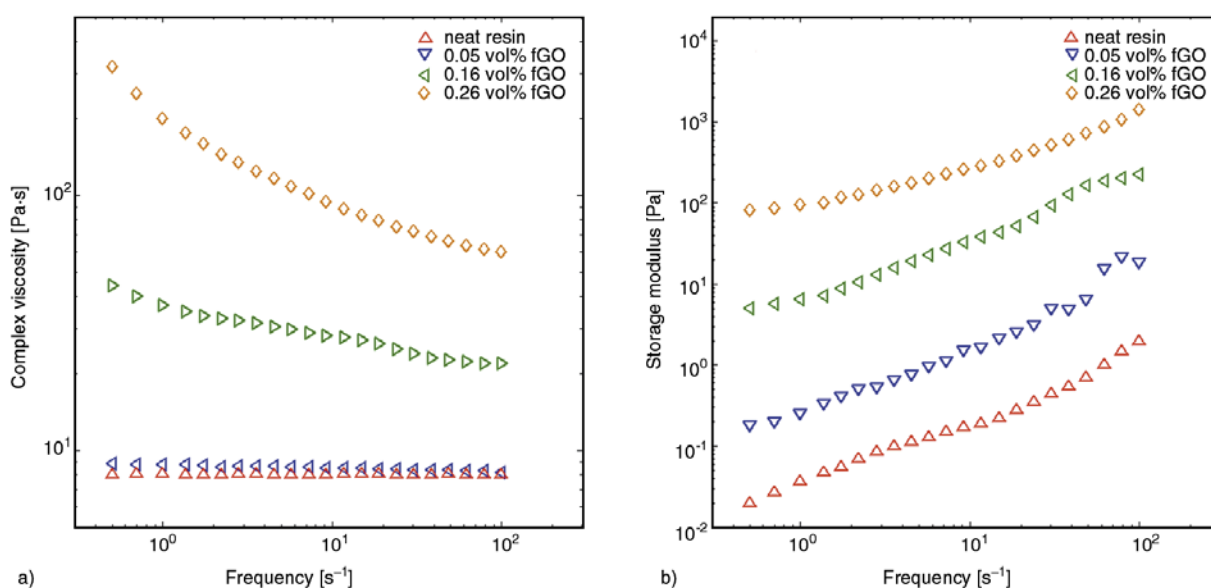


Figure 10. Results of rheometry for uncured epoxy-fGO mixtures with different fGO content (0 to 0.26 vol%) as a function of frequency at room temperature (a) complex viscosity and (b) storage modulus

increases and dependency on frequency decreases as fGO concentration increases and reaches a plateau for 0.26 vol% mixtures, showing solid-like flow behavior. These transitions in flow properties of resin upon addition of fGO are typical when a percolating network exists [51]. In other words, such behavior was an indication of network formation involving assembly of single nanolayers into a 3D network at very low concentration [53].

Therefore, the percolation threshold of the mixture is between 0.16 and 0.26 vol%. Such a low percolation threshold is strong evidence for excellent homogenous dispersion of monolayers throughout the matrix. Surprisingly, the obtained value for percolation threshold agrees very well with the predicted one (~0.2 vol%), substantiating the dispersion of monolayers, namely molecular level dispersion [11].

Recent studies on polymer-graphene nanocomposites have reported percolation thresholds, electrical or rheological, higher than theoretical values [54–57]. The use of melt mixing and even solution mixing of graphene sheets in different polymer matrices has resulted in a percolation threshold of 0.5 to 1 vol% of graphene [54–57]. An exceptionally low percolation threshold of epoxy-fGO composite, which is competitive with solution processed polymer-graphene, is an evidence for success of this method in dispersion of graphenic sheets [11].

3.4. Tensile properties

Mechanical properties of composites containing fGO were also studied in order to evaluate the effect of functionalization on the final composites. Figure 11 shows typical stress-strain curves from three points bending test. Flexural modulus of epoxy increased monotonically by addition of fGO and increased from 2800 ± 25 MPa (neat resin) to 3670 ± 60 MPa for composites containing 0.4 vol% fGO. In addition, ultimate flexural stresses increased by addition of graphenic nanosheets reaching up to 170 MPa after addition of 0.4 vol% fGO while strain to break shows marginal decrease at all fGO content. These notable enhancements in the mechanical properties of the epoxy-fGO composites can be attributed to strong bonding of nanosheets and matrix arising from covalent bonding between them and also fine dispersion of graphene layers through the matrix. However, compared with the neat epoxy,

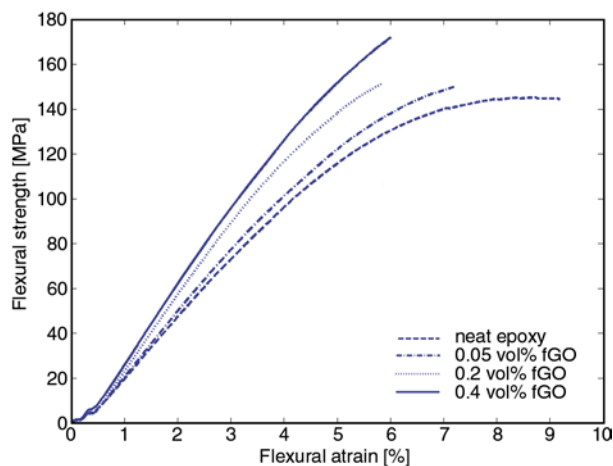


Figure 11. Typical flexural strength versus strain curves for neat resin and composites containing different fGO content

one can find just about a 30 and 12% increase in Young's modulus and ultimate strength by addition of 0.4 vol% fGO, respectively.

From composite science point of view, reinforcing a stiff matrix is more difficult rather than a soft polymer. As a result, comparing the relative enhancement of mechanical properties is not a fair way. Reasonable comparison can be performed through the calculating the reinforcing efficiency of reinforcing phase, *i.e.* graphene. One can estimate the mechanical properties of a composite material according rule of mixture as Equation (1) [58]:

$$Y_c = \varepsilon \cdot Y_f \varphi + Y_m(1 - \varphi) \quad (1)$$

where Y is mechanical property (modulus or strength) of composite, filler or matrix and φ is volume fraction (Equation 1). ε is reinforcing efficiency factor and therefore $0 < \varepsilon < 1$. In fact, $\varepsilon \cdot Y_f$ can be considered as efficient mechanical property of filler which is sensed by matrix. This parameter represents the efficiency of filler as reinforcing phase and is a good measure of comparing the composite systems having similar filler. At low filler content (Equation (2)):

$$\varepsilon \cdot Y_f \approx \frac{Y_c - Y_m}{\varphi} \quad (2)$$

In our system, efficient modulus and strength of graphene therefore is about 217 and 7.5 GPa (at volume fraction of 0.4 vol%), respectively (Equation (2)). Figure 12a shows comparison of this

parameter in different polymer-graphene systems prepared with various methods. The results obtained in this study are located at top fraction of those calculated from literature [12, 28, 29, 59–70], reflecting the superior performance of developed method to incorporate graphene in thermoset matrix.

Apart from effective stiffening of epoxy resin, no limitation in reinforcing of matrix was observed by increasing the graphene content except thickening of resin whereas degradation in use of nanofiller as stiffening phase at high loading is quite common. For epoxy-graphene nanocomposites, Rafiee *et al.* [27] found remarkable enhancement in tensile properties of epoxy after addition of less than 0.125 wt% functionalized graphene (50% in Young’s modulus and ~45% in ultimate strength) whereas tensile properties dropped to even lower than baseline epoxy after addition of 0.5 wt% graphene. In their recent work on epoxy-graphene nanoribbon nanocomposites, similar degradation in the performance of graphene for reinforcing epoxy has been observed after the addition of just 0.3 wt% graphene nanoribbon [71]. In our case, no degradation is observed in the superior performance of graphene sheets for reinforcing polymer matrix which is based on strong interaction of filler and matrix and molecular level dispersion of fGO sheets through the epoxy matrix.

The Halpin-Tsai model is widely used to calculate the modulus of nanocomposites containing platelet or fibril like fillers [72]. For a randomly distributed

platelet with modulus of E_f in a matrix with modulus of E_m , the modulus of a composite containing φ vol% of filler is estimated as Equation (3):

$$\frac{E}{E_m} = \frac{1 + 2\alpha\eta\varphi}{1 - \eta\varphi} \tag{3}$$

where α is the aspect ratio of platelet and η is given as Equation (4):

$$\eta = \frac{\frac{E_f}{E_m} - 1}{\frac{E_f}{E_m} + 2\alpha} \tag{4}$$

Considering the modulus of chemically derived graphene to be roughly 250 GPa [73], and an average aspect ratio of 350 for fGO sheets, the theoretical modulus of composites can be calculated as a function of graphene content (Equations (3) and (4)). Figure 12b shows theoretical modulus of composites compared with the experimental data. The close agreement between theoretical predictions and experimental measurements further confirms that graphene is indeed dispersed as single layers with a strong bond to the resin which has resulted in perfect load transfer to graphene sheets. If the aspect ratio of fGO considered lower than one for GO (350) due to the short sonication (10 minutes) for homogenization, the theoretical prediction would be lower than experimental results which is usually attributed to the formation of a stiffened interphase [58].

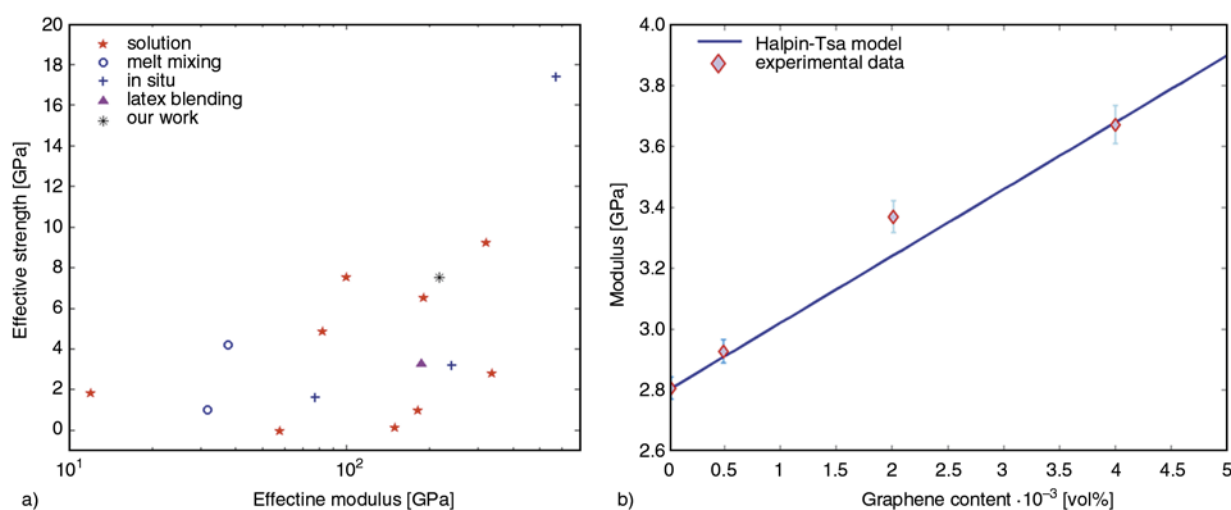


Figure 12. (a) Comparison of effective modulus and strength of graphene in polymer-graphene composites fabricated through different methods [12, 28, 29, 59–70] and the result obtained in this study. (b) Young’s modulus of epoxy composites as a function of graphene content. The line illustrates Halpin-Tsai prediction for Young’s modulus of composites containing ellipsoids with random dispersion as a function of graphene volume fraction showing agreement of theoretical prediction and experimental data.

Finally, it is worth noting that the above analysis shows that there is still large room for improving final mechanical properties and possibly other properties of nanocomposites by using graphene with larger aspect ratio and higher content. However, high viscosity of highly filled epoxy-graphene nanocomposites challenges the processing and application. Interfacial interaction of graphene and matrix can also be tuned by using amines with different molecular stiffness [28]. We believe this work paves the way for production of highly dispersed epoxy-graphene nanocomposites using a general approach.

4. Conclusions

The application of a two phase reacting system for functionalization of graphene oxide is shown to result in a very ideal graphene epoxy composite. It is ideal in the sense that graphene sheets are well dispersed to single layers and have very good bonding with the epoxy. It is observed that good dispersion and bonding can be maintained up to 0.5 vol% (~1 wt%). Therefore, functionalization of GO using the two phase method has served three purposes that are all important in improvement of epoxy-graphene composite; increasing the graphene content while maintaining good dispersion and furnishing good bonding between graphene and epoxy.

Acknowledgements

The authors wish to thank Mrs. Jalilzade from Maharfan Abzar Co. for help in AFM measurements.

References

- [1] Kroto H. W., Heath J. R., O'Brien S. C., Curl R. F., Smalley R. E.: C₆₀: Buckminsterfullerene. *Nature*, **318**, 162–163 (1985).
DOI: [10.1038/318162a0](https://doi.org/10.1038/318162a0)
- [2] Iijima S.: Helical microtubules of graphitic carbon. *Nature*, **354**, 56–58 (1991).
DOI: [10.1038/354056a0](https://doi.org/10.1038/354056a0)
- [3] Geim A. K., Novoselov K. S.: The rise of graphene. *Nature Materials*, **6**, 183–191 (2007).
DOI: [10.1038/nmat1849](https://doi.org/10.1038/nmat1849)
- [4] Coleman J. N., Khan U., Blau W. J., Gun'ko Y. K.: Small but strong: A review of the mechanical properties of carbon nanotube-polymer composites. *Carbon*, **44**, 1624–1652 (2006).
DOI: [10.1016/j.carbon.2006.02.038](https://doi.org/10.1016/j.carbon.2006.02.038)
- [5] Potts J. R., Dreyer D. R., Bielawski C. W., Ruoff R. S.: Graphene-based polymer nanocomposites. *Polymer*, **52**, 5–25 (2011).
DOI: [10.1016/j.polymer.2010.11.042](https://doi.org/10.1016/j.polymer.2010.11.042)
- [6] Liu Q., Liu Z., Zhang X., Yang L., Zhang N., Pan G., Yin S., Chen Y., Wei J.: Polymer photovoltaic cells based on solution-processable graphene and P3HT. *Advanced Functional Materials*, **19**, 894–904 (2009).
DOI: [10.1002/adfm.200800954](https://doi.org/10.1002/adfm.200800954)
- [7] Li N., Huang Y., Du F., He X., Lin X., Gao H., Ma Y., Li F., Chen Y., Eklund P. C.: Electromagnetic interference (EMI) shielding of single-walled carbon nanotube epoxy composites. *Nano Letters*, **6**, 1141–1145 (2006).
DOI: [10.1021/nl0602589](https://doi.org/10.1021/nl0602589)
- [8] Kauffman D. R., Star A.: Carbon nanotube gas and vapor sensors. *Angewandte Chemie International Edition*, **47**, 6550–6570 (2008).
DOI: [10.1002/anie.200704488](https://doi.org/10.1002/anie.200704488)
- [9] Baughman R. H., Zakhidov A. A., de Heer W. A.: Carbon nanotubes – The route toward applications. *Science*, **297**, 787–792 (2002).
DOI: [10.1126/science.1060928](https://doi.org/10.1126/science.1060928)
- [10] Du J.-H., Bai J., Cheng H.-M.: The present status and key problems of carbon nanotube based polymer composites. *Express Polymer Letters*, **1**, 253–273 (2007).
DOI: [10.3144/expresspolymlett.2007.39](https://doi.org/10.3144/expresspolymlett.2007.39)
- [11] Stankovich S., Dikin D. A., Dommett G. H. B., Kohlhaas K. M., Zimney E. J., Stach E. A., Piner R. D., Nguyen S. T., Ruoff R. S.: Graphene-based composite materials. *Nature*, **442**, 282–286 (2006).
DOI: [10.1038/nature04969](https://doi.org/10.1038/nature04969)
- [12] Ramanathan T., Abdala A. A., Stankovich S., Dikin D. A., Herrera-Alonso M., Piner R. D., Adamson D. H., Schniepp H. C., Chen X., Ruoff R. S., Nguyen S. T., Aksay I. A., Prud'Homme R. K., Brinson L. C.: Functionalized graphene sheets for polymer nanocomposites. *Nature Nanotechnology*, **3**, 327–331 (2008).
DOI: [10.1038/nnano.2008.96](https://doi.org/10.1038/nnano.2008.96)
- [13] Tjong S. C.: Graphene and its derivatives: Novel materials for forming functional polymer nanocomposites. *Express Polymer Letters*, **6**, 437 (2012).
DOI: [10.3144/expresspolymlett.2012.46](https://doi.org/10.3144/expresspolymlett.2012.46)
- [14] Park S., Ruoff R. S.: Chemical methods for the production of graphenes. *Nature Nanotechnology*, **4**, 217–224 (2009).
DOI: [10.1038/nnano.2009.58](https://doi.org/10.1038/nnano.2009.58)
- [15] Li D., Müller M. B., Gilje S., Kaner R. B., Wallace G. G.: Processable aqueous dispersions of graphene nanosheets. *Nature Nanotechnology*, **3**, 101–105 (2008).
DOI: [10.1038/nnano.2007.451](https://doi.org/10.1038/nnano.2007.451)
- [16] Pan S., Aksay I. A.: Factors controlling the size of graphene oxide sheets produced *via* the graphite oxide route. *ACS Nano*, **5**, 4073–4083 (2011).
DOI: [10.1021/nn200666r](https://doi.org/10.1021/nn200666r)
- [17] Gudarzi M. M., Sharif F.: Characteristics of polymers that stabilize colloids for the production of graphene from graphene oxide. *Journal of Colloid and Interface Science*, **349**, 63–69 (2010).
DOI: [10.1016/j.jcis.2010.05.064](https://doi.org/10.1016/j.jcis.2010.05.064)

- [18] Qiu S. L., Wang C. S., Wang Y. T., Liu C. G., Chen X. Y., Xie H. F., Huang Y. A., Cheng R. S.: Effects of graphene oxides on the cure behaviors of a tetrafunctional epoxy resin. *Express Polymer Letters*, **5**, 809–818 (2011).
DOI: [10.3144/expresspolymlett.2011.79](https://doi.org/10.3144/expresspolymlett.2011.79)
- [19] Lomeda J. R., Doyle C. D., Kosynkin D. V., Hwang W-F., Tour J. M.: Diazonium functionalization of surfactant-wrapped chemically converted graphene sheets. *Journal of the American Chemical Society*, **130**, 16201–16206 (2008).
DOI: [10.1021/ja806499w](https://doi.org/10.1021/ja806499w)
- [20] Allen M. J., Tung V. C., Kaner R. B.: Honeycomb carbon: A review of graphene. *Chemical Reviews*, **110**, 132–145 (2010).
DOI: [10.1021/cr900070d](https://doi.org/10.1021/cr900070d)
- [21] Tkalya E., Ghislandi M., Alekseev A., Koning C., Loos J.: Latex-based concept for the preparation of graphene-based polymer nanocomposites. *Journal of Materials Chemistry*, **20**, 3035–3039 (2010).
DOI: [10.1039/B922604D](https://doi.org/10.1039/B922604D)
- [22] Gudarzi M. M., Sharif F.: Molecular level dispersion of graphene in polymer matrices using colloidal polymer and graphene. *Journal of Colloid and Interface Science*, **366**, 44–50 (2012).
DOI: [10.1016/j.jcis.2011.09.086](https://doi.org/10.1016/j.jcis.2011.09.086)
- [23] Yousefi N., Gudarzi M. M., Zheng Q., Aboutalebi S. H., Sharif F., Kim J-K.: Self-alignment and high electrical conductivity of ultralarge graphene oxide–polyurethane nanocomposites. *Journal of Materials Chemistry*, **22**, 12709–12717 (2012).
DOI: [10.1039/c2jm30590a](https://doi.org/10.1039/c2jm30590a)
- [24] Yoonessi M., Gaier J. R.: Highly conductive multifunctional graphene polycarbonate nanocomposites. *ACS Nano*, **4**, 7211–7220 (2010).
DOI: [10.1021/nn1019626](https://doi.org/10.1021/nn1019626)
- [25] Gudarzi M. M., Sharif F.: Self assembly of graphene oxide at the liquid–liquid interface: A new route to the fabrication of graphene based composites. *Soft Matter*, **7**, 3432–3440 (2011).
DOI: [10.1039/C0SM01311K](https://doi.org/10.1039/C0SM01311K)
- [26] Yang H., Shan C., Li F., Zhang Q., Han D., Niu L.: Convenient preparation of tunably loaded chemically converted graphene oxide/epoxy resin nanocomposites from graphene oxide sheets through two-phase extraction. *Journal of Materials Chemistry*, **19**, 8856–8860 (2009).
DOI: [10.1039/B915228H](https://doi.org/10.1039/B915228H)
- [27] Rafiee M. A., Rafiee J., Srivastava I., Wang Z., Song H., Yu Z-Z., Koratkar N.: Fracture and fatigue in graphene nanocomposites. *Small*, **6**, 179–183 (2009).
DOI: [10.1002/smll.200901480](https://doi.org/10.1002/smll.200901480)
- [28] Fang M., Zhang Z., Li J., Zhang H., Lu H., Yang Y.: Constructing hierarchically structured interphases for strong and tough epoxy nanocomposites by amine-rich graphene surfaces. *Journal of Materials Chemistry*, **20**, 9635–9643 (2010).
DOI: [10.1039/C0JM01620A](https://doi.org/10.1039/C0JM01620A)
- [29] Bortz D. R., Heras E. G., Martin-Gullon I.: Impressive fatigue life and fracture toughness improvements in graphene oxide/epoxy composites. *Macromolecules*, **45**, 238–245 (2012).
DOI: [10.1021/ma201563k](https://doi.org/10.1021/ma201563k)
- [30] Wang S., Tambraparni M., Qiu J., Tipton J., Dean D.: Thermal expansion of graphene composites. *Macromolecules*, **42**, 5251–5255 (2009).
DOI: [10.1021/ma900631c](https://doi.org/10.1021/ma900631c)
- [31] Rafiee M. A., Rafiee J., Wang Z., Song H., Yu Z-Z., Koratkar N.: Enhanced mechanical properties of nanocomposites at low graphene content. *ACS Nano*, **3**, 3884–3890 (2009).
DOI: [10.1021/nn9010472](https://doi.org/10.1021/nn9010472)
- [32] Aboutalebi S. H., Gudarzi M. M., Zheng Q. B., Kim J-K.: Spontaneous formation of liquid crystals in ultralarge graphene oxide dispersions. *Advanced Functional Materials*, **21**, 2978–2988 (2011).
DOI: [10.1002/adfm.201100448](https://doi.org/10.1002/adfm.201100448)
- [33] Yang X., Zhu J., Qiu L., Li D.: Bioinspired effective prevention of restacking in multilayered graphene films: Towards the next generation of high-performance supercapacitors. *Advanced Materials*, **23**, 2833–2838 (2011).
DOI: [10.1002/adma.201100261](https://doi.org/10.1002/adma.201100261)
- [34] Yang X., Qiu L., Cheng C., Wu Y., Ma Z-F., Li D.: Ordered gelation of chemically converted graphene for next-generation electroconductive hydrogel films. *Angewandte Chemie – International Edition*, **50**, 7325–7328 (2011).
DOI: [10.1002/anie.201100723](https://doi.org/10.1002/anie.201100723)
- [35] Luo J., Jang H. D., Sun T., Xiao L., He Z., Katsoulidis A. P., Kanatzidis M. G., Gibson J. M., Huang J.: Compression and aggregation-resistant particles of crumpled soft sheets. *ACS Nano*, **5**, 8943–8949 (2011).
DOI: [10.1021/nn203115u](https://doi.org/10.1021/nn203115u)
- [36] Kim H., Abdala A. A., Macosko C. W.: Graphene/polymer nanocomposites. *Macromolecules*, **43**, 6515–6530 (2010).
DOI: [10.1021/ma100572e](https://doi.org/10.1021/ma100572e)
- [37] Hummers Jr W. S., Offeman R. E.: Preparation of graphitic oxide. *Journal of the American Chemical Society*, **80**, 1339 (1958).
DOI: [10.1021/ja01539a017](https://doi.org/10.1021/ja01539a017)
- [38] Gojny F. H., Wichmann M. H. G., Köpke U., Fiedler B., Schulte K.: Carbon nanotube-reinforced epoxy-composites: enhanced stiffness and fracture toughness at low nanotube content. *Composites Science and Technology*, **64**, 2363–2371 (2004).
DOI: [10.1016/j.compscitech.2004.04.002](https://doi.org/10.1016/j.compscitech.2004.04.002)
- [39] Shen J., Huang W., Wu L., Hu Y., Ye M.: The reinforcement role of different amino-functionalized multiwalled carbon nanotubes in epoxy nanocomposites. *Composites Science and Technology*, **67**, 3041–3050 (2007).
DOI: [10.1016/j.compscitech.2007.04.025](https://doi.org/10.1016/j.compscitech.2007.04.025)

- [40] Zheng Y., Zhang A., Chen Q., Zhang J., Ning R.: Functionalized effect on carbon nanotube/epoxy nano-composites. *Materials Science and Engineering A*, **435–436**, 145–149 (2006).
DOI: [10.1016/j.msea.2006.07.106](https://doi.org/10.1016/j.msea.2006.07.106)
- [41] Wang S., Chia P-J., Chua L-L., Zhao L-H., Png R-Q., Sivaramakrishnan S., Zhou M., Goh R-G. S., Friend R-H., Wee A. T-S., Ho P. K-H.: Band-like transport in surface-functionalized highly solution-processable graphene nanosheets. *Advanced Materials*, **20**, 3440–3446 (2008).
DOI: [10.1002/adma.200800279](https://doi.org/10.1002/adma.200800279)
- [42] Wang G., Shen X., Wang B., Yao J., Park J.: Synthesis and characterisation of hydrophilic and organophilic graphene nanosheets. *Carbon*, **47**, 1359–1364 (2009).
DOI: [10.1016/j.carbon.2009.01.027](https://doi.org/10.1016/j.carbon.2009.01.027)
- [43] Zaarei D., Sarabi A. A., Sharif F., Gudarzi M. M., Kassirha S. M.: Using of p-phenylenediamine as modifier of montmorillonite for preparation of epoxy-clay nanocomposites: Morphology and solvent resistance properties. *Polymer-Plastics Technology and Engineering*, **49**, 285–291 (2010).
DOI: [10.1080/03602550903413946](https://doi.org/10.1080/03602550903413946)
- [44] Park S., Dikin D. A., Nguyen S. T., Ruoff R. S.: Graphene oxide sheets chemically cross-linked by polyallylamine. *Journal of Physical Chemistry C*, **113**, 15801–15804 (2009).
DOI: [10.1021/jp907613s](https://doi.org/10.1021/jp907613s)
- [45] Chen Y., Zhang X., Yu P., Ma Y.: Stable dispersions of graphene and highly conducting graphene films: A new approach to creating colloids of graphene monolayers. *Chemical Communications*, **45**, 4527–4529 (2009).
DOI: [10.1039/B907723E](https://doi.org/10.1039/B907723E)
- [46] Ma J., Yu Z-Z., Zhang Q-X., Xie X-L., Mai Y-W., Luck I.: A novel method for preparation of disorderly exfoliated epoxy/clay nanocomposite. *Chemistry of Materials*, **16**, 757–759 (2004).
DOI: [10.1021/cm0349203](https://doi.org/10.1021/cm0349203)
- [47] Stelzig S. H., Klapper M., Müllen K.: A simple and efficient route to transparent nanocomposites. *Advanced Materials*, **20**, 929–932 (2008).
DOI: [10.1002/adma.200701608](https://doi.org/10.1002/adma.200701608)
- [48] Liang Y., Wu D., Feng X., Müllen K.: Dispersion of graphene sheets in organic solvent supported by ionic interactions. *Advanced Materials*, **21**, 1679–1683 (2009).
DOI: [10.1002/adma.200803160](https://doi.org/10.1002/adma.200803160)
- [49] Wei T., Luo G., Fan Z., Zheng C., Yan J., Yao C., Li W., Zhang C.: Preparation of graphene nanosheet/polymer composites using in situ reduction–extractive dispersion. *Carbon*, **47**, 2296–2299 (2009).
DOI: [10.1016/j.carbon.2009.04.030](https://doi.org/10.1016/j.carbon.2009.04.030)
- [50] Garboczi E. J., Snyder K. A., Douglas J. F., Thorpe M. F.: Geometrical percolation threshold of overlapping ellipsoids. *Physical Review E*, **52**, 819–828 (1995).
DOI: [10.1103/PhysRevE.52.819](https://doi.org/10.1103/PhysRevE.52.819)
- [51] Kharchenko S. B., Douglas J. F., Obrzut J., Grulke E. A., Milger K. B.: Flow-induced properties of nanotube-filled polymer materials. *Nature Materials*, **3**, 564–568 (2004).
DOI: [10.1038/nmat1183](https://doi.org/10.1038/nmat1183)
- [52] Sun L., Boo W-J., Liu J., Clearfield A., Sue H-J., Verghese N. E., Pham H. Q., Bicerano J.: Effect of nanoplatelets on the rheological behavior of epoxy monomers. *Macromolecular Materials and Engineering*, **294**, 103–113 (2008).
DOI: [10.1002/mame.200800258](https://doi.org/10.1002/mame.200800258)
- [53] Zaarei D., Sarabi A. A., Sharif F., Kassirha S. M., Gudarzi M. M.: Rheological studies of uncured epoxy–organoclaynanocomposite coatings. *e-Polymers*, no.117 (2008).
- [54] Villar-Rodil S., Paredes J. I., Martínez-Alonso A., Tascón J. M. D.: Preparation of graphene dispersions and graphene-polymer composites in organic media. *Journal of Materials Chemistry*, **19**, 3591–3593 (2009).
DOI: [10.1039/B904935E](https://doi.org/10.1039/B904935E)
- [55] Kim H., Macosko C. W.: Processing-property relationships of polycarbonate/graphene composites. *Polymer*, **50**, 3797–3809 (2009).
DOI: [10.1016/j.polymer.2009.05.038](https://doi.org/10.1016/j.polymer.2009.05.038)
- [56] Raghu A. V., Lee Y. R., Jeong H. M., Shin C. M.: Preparation and physical properties of waterborne polyurethane/functionalized graphene sheet nanocomposites. *Macromolecular Chemistry and Physics*, **209**, 2487–2493 (2008).
DOI: [10.1002/macp.200800395](https://doi.org/10.1002/macp.200800395)
- [57] Liang J., Wang Y., Huang Y., Ma Y., Liu Z., Cai J., Zhang C., Gao H., Chen Y.: Electromagnetic interference shielding of graphene/epoxy composites. *Carbon*, **47**, 922–925 (2009).
DOI: [10.1016/j.carbon.2008.12.038](https://doi.org/10.1016/j.carbon.2008.12.038)
- [58] Coleman J. N., Cadek M., Blake R., Nicolosi V., Ryan K. P., Belton C., Fonseca A., Nagy J. B., Gun'ko Y. K., Blau W. J.: High performance nanotube-reinforced plastics: Understanding the mechanism of strength increase. *Advanced Functional Materials*, **14**, 791–798 (2004).
DOI: [10.1002/adfm.200305200](https://doi.org/10.1002/adfm.200305200)
- [59] Liang J., Huang Y., Zhang L., Wang Y., Ma Y., Guo T., Chen Y.: Molecular-level dispersion of graphene into poly(vinyl alcohol) and effective reinforcement of their nanocomposites. *Advanced Functional Materials*, **19**, 2297–2302 (2009).
DOI: [10.1002/adfm.200801776](https://doi.org/10.1002/adfm.200801776)
- [60] Kim H., Macosko C. W.: Morphology and properties of polyester/exfoliated graphite nanocomposites. *Macromolecules*, **41**, 3317–3327 (2008).
DOI: [10.1021/ma702385h](https://doi.org/10.1021/ma702385h)
- [61] Vadukumpully S., Paul J., Mahanta N., Valiyaveettil S.: Flexible conductive graphene/poly(vinyl chloride) composite thin films with high mechanical strength and thermal stability. *Carbon*, **49**, 198–205 (2011).
DOI: [10.1016/j.carbon.2010.09.004](https://doi.org/10.1016/j.carbon.2010.09.004)

- [62] Zhao X., Zhang Q., Chen D., Lu P.: Enhanced mechanical properties of graphene-based poly(vinyl alcohol) composites. *Macromolecules*, **43**, 2357–2363 (2010). DOI: [10.1021/ma902862u](https://doi.org/10.1021/ma902862u)
- [63] Yang S-Y., Lin W-N., Huang Y-L., Tien H-W., Wang J-Y., Ma C-C. M., Li S-M., Wang Y-S.: Synergetic effects of graphene platelets and carbon nanotubes on the mechanical and thermal properties of epoxy composites. *Carbon*, **49**, 793–803 (2010). DOI: [10.1016/j.carbon.2010.10.014](https://doi.org/10.1016/j.carbon.2010.10.014)
- [64] Wang Y., Shi Z., Fang J., Xu H., Yin J.: Graphene oxide/polybenzimidazole composites fabricated by a solvent-exchange method. *Carbon*, **49**, 1199–1207 (2011). DOI: [10.1016/j.carbon.2010.11.036](https://doi.org/10.1016/j.carbon.2010.11.036)
- [65] Rafiq R., Cai D., Jin J., Song M.: Increasing the toughness of nylon 12 by the incorporation of functionalized graphene. *Carbon*, **48**, 4309–4314 (2010). DOI: [10.1016/j.carbon.2010.07.043](https://doi.org/10.1016/j.carbon.2010.07.043)
- [66] Song P., Cao Z., Cai Y., Zhao L., Fang Z., Fu S.: Fabrication of exfoliated graphene-based polypropylene nanocomposites with enhanced mechanical and thermal properties. *Polymer*, **52**, 4001–4010 (2011). DOI: [10.1016/j.polymer.2011.06.045](https://doi.org/10.1016/j.polymer.2011.06.045)
- [67] Potts J. R., Lee S. H., Alam T. M., An J., Stoller M. D., Piner R. D., Ruoff R. S.: Thermomechanical properties of chemically modified graphene/poly(methyl methacrylate) composites made by *in situ* polymerization. *Carbon*, **49**, 2615–2623 (2011). DOI: [10.1016/j.carbon.2011.02.023](https://doi.org/10.1016/j.carbon.2011.02.023)
- [68] Yun Y. S., Bae Y. H., Kim D. H., Lee J. Y., Chin I-J., Jin H-J.: Reinforcing effects of adding alkylated graphene oxide to polypropylene. *Carbon*, **49**, 3553–3559 (2011). DOI: [10.1016/j.carbon.2011.04.055](https://doi.org/10.1016/j.carbon.2011.04.055)
- [69] Chen D., Zhu H., Liu T.: In situ thermal preparation of polyimide nanocomposite films containing functionalized graphene sheets. *ACS Applied Materials and Interfaces*, **3**, 3702–3708 (2011). DOI: [10.1021/am1008437](https://doi.org/10.1021/am1008437)
- [70] Gonçalves G., Marques P., Barros-Timmons A., Bdkin I., Singh M. K., Emami N., Grácio J.: Graphene oxide modified with PMMA *via* ATRP as a reinforcement filler. *Journal of Materials Chemistry*, **20**, 9927–9934 (2010). DOI: [10.1039/c0jm01674h](https://doi.org/10.1039/c0jm01674h)
- [71] Rafiee M. A., Lu W., Thomas A. V., Zandiatashbar A., Rafiee J., Tour J. M., Koratkar N. A.: Graphene nanoribbon composites. *ACS Nano*, **4**, 7415–7420 (2010). DOI: [10.1021/nn102529n](https://doi.org/10.1021/nn102529n)
- [72] Wu Y-P., Jia Q-X., Yu D-S., Zhang L-Q.: Modeling Young's modulus of rubber-clay nanocomposites using composite theories. *Polymer Testing*, **23**, 903–909 (2004). DOI: [10.1016/j.polymertesting.2004.05.004](https://doi.org/10.1016/j.polymertesting.2004.05.004)
- [73] Gómez-Navarro C., Burghard M., Kern K.: Elastic properties of chemically derived single graphene sheets. *Nano Letters*, **8**, 2045–2049 (2008). DOI: [10.1021/nl801384y](https://doi.org/10.1021/nl801384y)